MASTER

RESEARCH PROPOSAL

GEORGIA INSTITUTE OF TECHNOLOGY

1885

Atlanta, Georgia 30332

Contracting Through
Georgia Tech Research Institute

AS05-78ER06030

A KINETIC STUDY OF
RADICAL - AROMATIC HYDROCARBON REACTIONS

Annual Progress Report No. 3

May 1, 1980 — March 31, 1981

Submitted to:

The Division of Basic Energy Sciences
Department of Energy
Washington, D.C. 20545

By:

Molecular Sciences Group
Engineering Experiment Station
Georgia Institute of Technology
Atlanta, Georgia 30332

Principal Investigagor:

Dr. A.R. Ravishankara

April 3, 1981

DISTRIBUTION OF THIS DOCUMENT IS UNLIMITED

MGW

A KINETIC STUDY OF RADICAL-AROMATIC HYDROCARBON REACTIONS

Annual Progress Report No. 3
(May 1, 1980—March 31, 1981)

In the previous progress report we described our studies of OH reactions with benzene, toluene, and their isotopic analogs. This work is now in press to be published in the Journal of Physical Chemistry. A copy of preprint is attached as Appendix 1. removed

During the last 12 months, the analysis of some of the data on reactions with benzene and toluenes were completed (see Appendix 1). The following OH reactions were also studied:

OH + o-xylene → products 298-970 K
OH + m-xylene → products 250-970 K
OH + p-xylene → products 298-970 K .

This work is now complete and has been written up for publication in the Journal of Physical Chemistry and is attached to this report as Appendix 2. removed Therefore, it will not be described further.

Apart from the above mentioned OH reactions, the following $O(^3P)$ reactions have been studied:

$O(^3P) + C_6H_6 \rightarrow$ products 298-870 K (1)
$O(^3P) + C_6D_6 \rightarrow$ products 298-806 K (2)
$O(^3P) + C_6H_5CH_3 \rightarrow$ products 298-930 K (3)
$O(^3P) + C_6H_5CD_3 \rightarrow$ products 298-930 K (4)
$O(^3P)$ + o-xylene → products 298-970 K (5)
$O(^3P)$ + m-xylene → products 298-970 K (6)
$O(^3P)$ + p-xylene → products 298-970 K (7)

A KINETICS STUDY OF THE REACTION OF $O(^3P)$ WITH AROMATIC HYDROCARBONS

EXPERIMENTAL

The utilization of the flash photolysis-resonance fluorescence technique in the study of $O(^3P)$ atom reaction kinetics is well established and is amply described in the literature. Recently, we have extended the temperature range of applicability of this method to permit rate constant measurements to be made at ∿ 1000 K.

A schematic diagram of the experimental apparatus is shown in Figure 1. The principal system components are (1) a thermostated quartz reaction cell equipped with long arms connected to O-ring joints via air-cooled jackets, (2) a spark discharge lamp perpendicular to one face of the cell, (3) a cw atomic oxygen resonance lamp perpendicular to the flashlamp, (4) a solar-blind photomultiplier tube perpendicular to both the photolysis and resonance radiation beams, and (5) a signal averager and fast photon counting electronics.

The all quartz reaction cell was resistively heated using electrically insulated nichrome wire windings mounted on its outer surface. This heating element was covered with ceramic felt and five layers of stainless steel radiation shields. The temperature of the gaseous mixture inside the reactor was directly measured using a retractable chromel alumel thermocouple introduced into the reactor through a cajon seal. The temperature gradient across the reaction zone (∿ 2 cm) was found to be ∿ 20 K at 1000 K and negligible at 500 K.

This cell is equipped with five air-cooled jackets which are attached to O-ring joints which hold the window material. The resonance lamp window was equipped with a CaF_2 window while the flashlamp window was made of

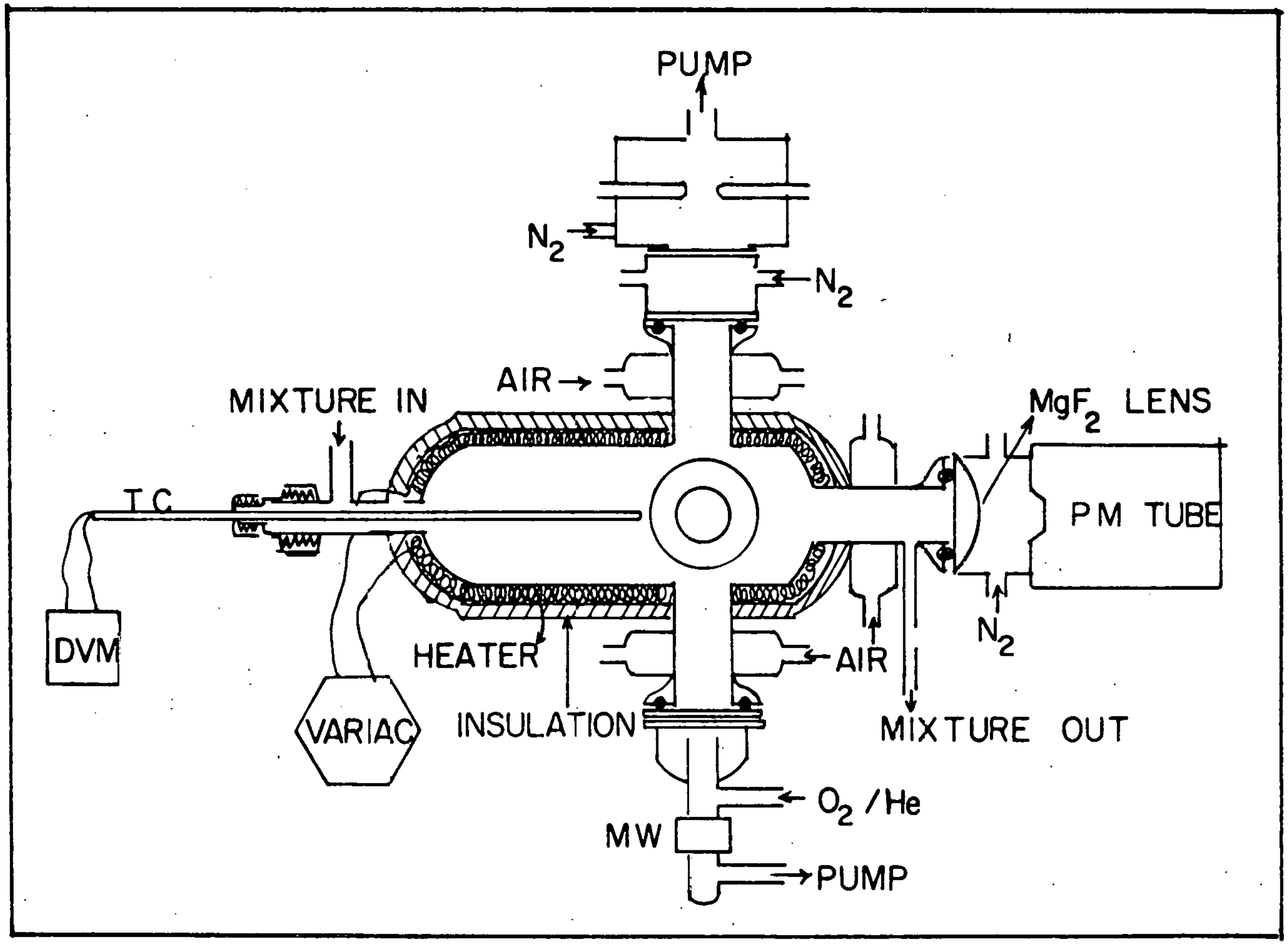

Figure 1. Schematic Diagram of the High Temperature Flash Photolysis-Resonance Fluorescence Apparatus used for $O(^3P)$ Reaction Studies.

sapphire; all the rest were made of quartz except the resonance light collection port which had an MgF_2 lens. The presence of air-cooled jackets enabled us to use O-ring joints to attach windows to the cell and keep the window material at room temperature, thereby greatly increasing the signal level as well as the ease of operation.

In all of the experiments discussed below, $O(^3P)$ atoms were produced by flash photolysis of O_2 at wavelengths between the sapphire cutoff at 145 nm and the onset of continuum absorption at 185 nm (flash duration $\leq$ 50μsec). Following the flash, oxygen atom resonance radiation continuously excited a small fraction of the $O(^3P)$ created in the reactor to its electronically excited state; the resultant fluorescence emanating in the direction perpendicular to both the resonance excitation and photolysis beams was collected by a lens and focused onto a solar-blind photolultiplier tube. Signals were obtained by photon counting and then fed into a signal averager operated in the multichannel scaling mode. For each decay rate measured, sufficient flashes were averaged to construct a well-defined temperal profile over at least a factor of twenty variation in $[O(^3P)]$.

All experiments were carried out under pseudo-first order kinetic conditions with the aromatic hydrocarbon concentration [RH] in excess, $[RH]/[O(^3P)] > 1000$. In the absence of secondary reactions which significantly deplete or reform the transient $O(^3P)$ species, $[O(^3P)]$ varies in an exponential manner with time:

$$[O(^3P)]_t = [O(^3P)]_0 \, e^{-(k[RH] + k_d)t} = [O(^3P)]_0 \, e^{-k't} \qquad (I)$$

where k' is the measured pseudo-first order rate constant, k is the bimolecular rate constant for the reaction

$$O(^3P) + RH \xrightarrow{k} \text{products} \; ,$$

[RH] is the (constant) aromatic hydrocarbon concentration, and k_d is the first order rate constant for $O(^3P)$ disappearance due to diffusion and reaction with O_2 in the absence of RH. Exponential $[O(^3P)]$ decays such as those displayed in Figure 2 (for reaction with benzene) were observed. k' values were taken as the slopes of such decays. RH concentration variations over a factor of at least ten led to k' vs. [RH] plots of the type shown in Figure 3 for 484 K. Bimolecular reaction rate constants k(T) were obtained as the slope of the least squares straight line through the (k', [RH]) data points.

In order to avoid the accumulation of photolysis or reaction products and to minimize any uncertainties in [RH] arising from aromatic hydrocarbon absorption on the reaction walls, all experiments were carried out under "slow flow" conditions. The flow rate through the cell was such that each photolysis flash encountered a fresh reaction mixture (photolysis repetition rate ∿ 0.5 Hz). The aromatic hydrocarbon RH was taken from a 12 ℓ bulb containing an RH/diluent gas mixture. The RH/diluent gas mixture, O_2 and additional diluent gas were mixed prior to entering the reaction cell. Concentrations of each component in the reaction mixture were determined from measurements of the appropriate mass flow rates (measured using calibrated mass flow meters) and the total pressure. The fraction of aromatic hydrocarbon in the RH/diluent gas mixture was checked frequently by simultaneous measurements of the aromatic hydrocarbon absorption at 253.7 nm and the total pressure of the mixture. These determinations were carried out using a Hg pen-ray lamp as the light source, an 80 cm long absorption cell, and a photomultiplier tube fitted with a bandpass filter. The absorption cross sections at 253.7 nm used to calculate the RH concentrations in the source mixtures were measured during the course of the experiments; the obtained values are: C_6H_6, 3.67×10^{-19} cm^2; C_6D_6, 2.39×10^{-19} cm^2; $C_6H_5CH_3$, 4.78×10^{-19} cm^2; $C_6H_5CD_3$, 5.26×10^{-19} cm^2; o-xylene, 5.98×10^{-19} cm^2;

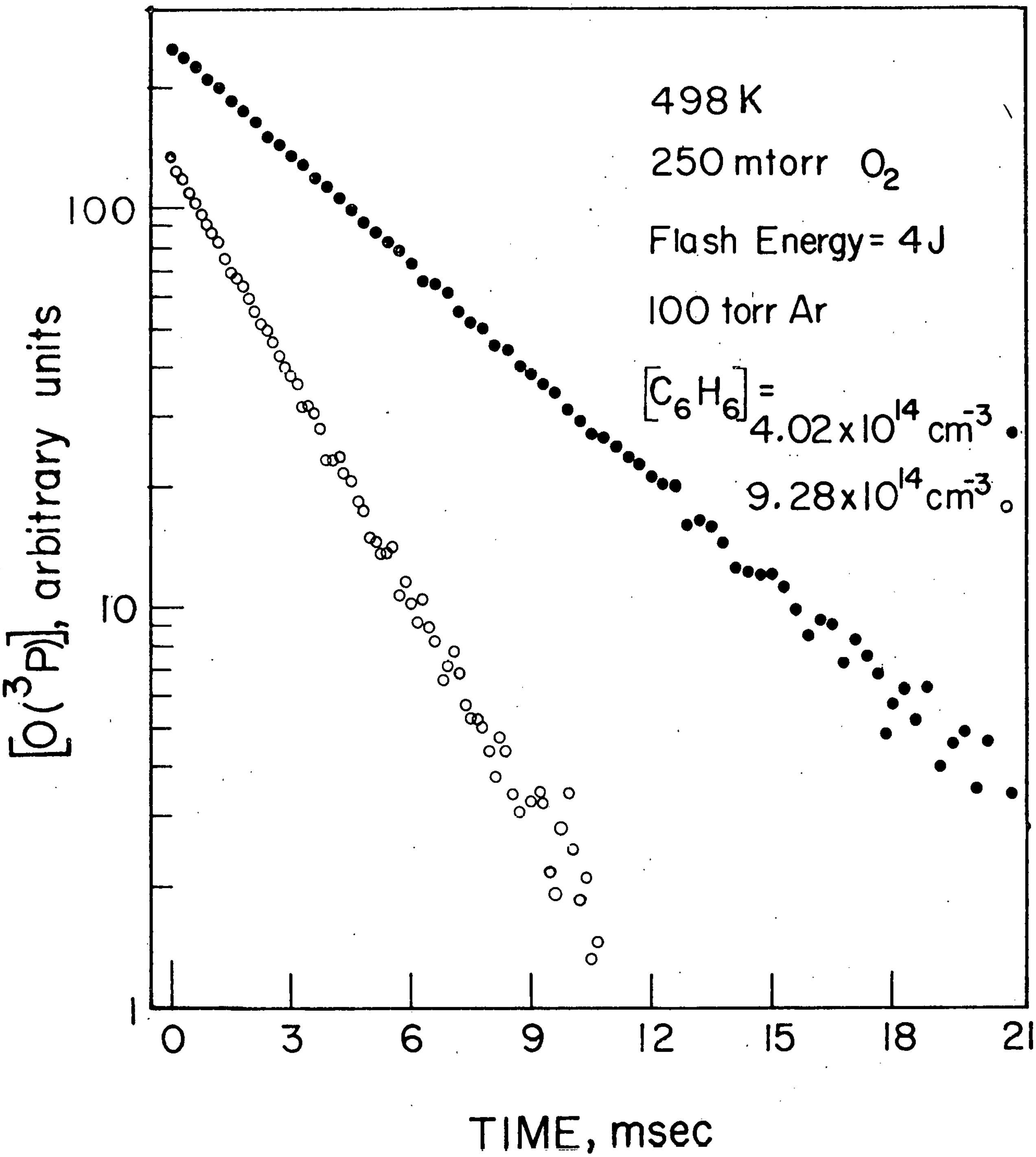

Figure 2. Temporal Profiles of $[O(^3P)]$ Following Photolysis of a Mixture of O_2, C_6H_6, and Ar. Experimental conditions are shown in the figure.

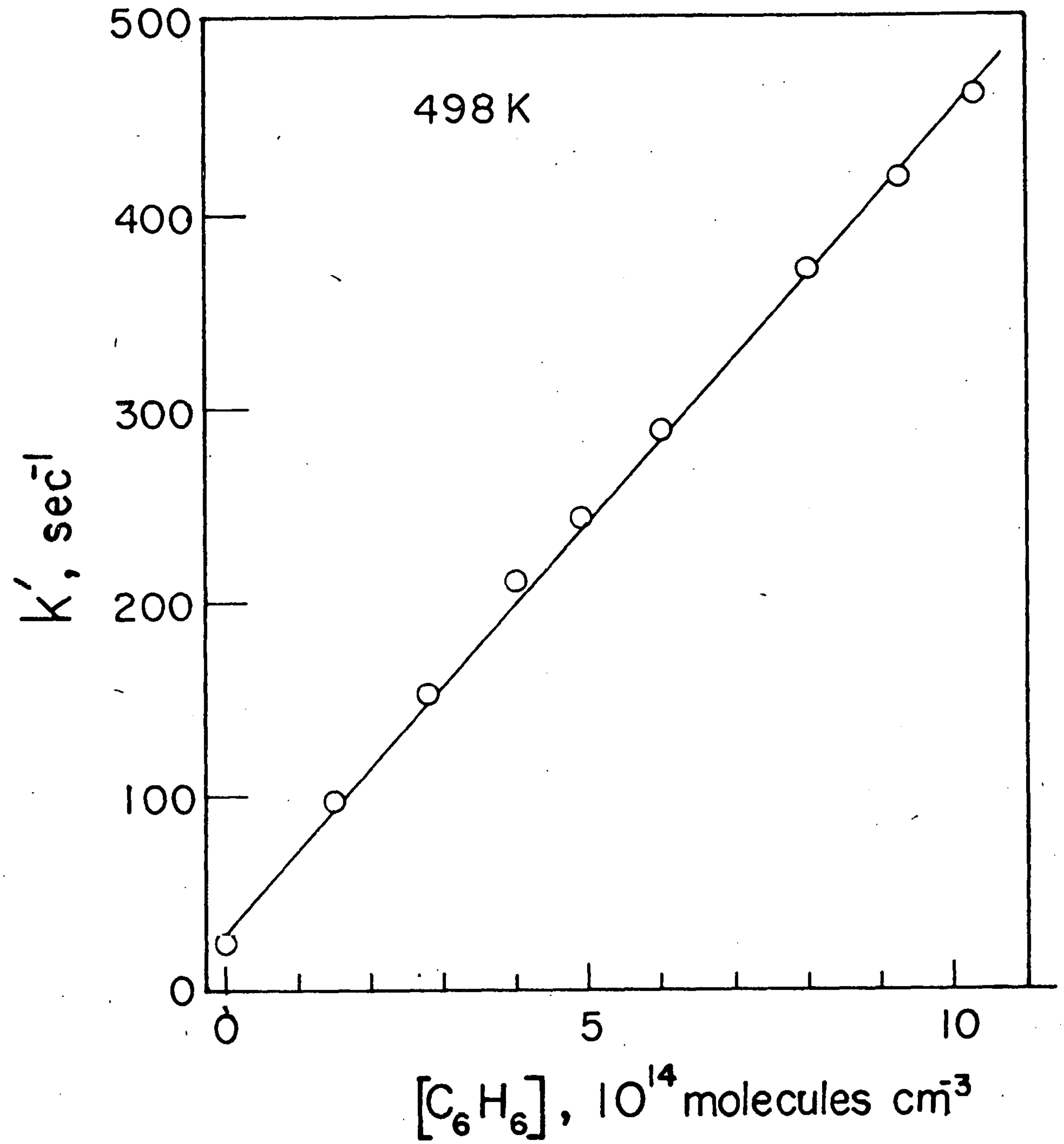

Figure 3. Plot of Pseudo First Order Rate Constant vs. $[C_6H_6]$ Concentration at 498 K.

m-xylene, 5.22 x 10^{-19} cm^2; and p-xylene, 6.16 x 10^{-19} cm^2. These cross sections and the resulting absolute [RH] values quoted for each experiment are accurate to 8%.

The bulb gases used in this study had the following stated purities: Ar > 99.9995%, He > 99.9999%, O_2 > 99.99%, N_2 > 99.9995%. Benzene, toluene and p-xylene were obtained from J. T. Baker, Co. and had analyzed purities of > 99.99%. The deuterated aromatics were purchased from Merck, Sharpe, and Dohme, Canada, Ltd. Their chemical purity was > 99.99% and their selectively labelled isotopic purities were as follows: C_6D_6 > 99.96% D and $C_6H_5CD_3$ > 99.0% D. O-xylene and m-xylene were obtained from Eastman Co. and their purity level was greater than 99.9%. All aromatic hydrocarbons were degased before use.

RESULTS

The rate constants obtained in this study for reactions (1)-(4) and reactions (5)-(7) are listed in tabular form in Tables I and II, respectively. Figure 4 shows the results of reactions 1 and 2 is an Arrhenius plot while similar plots are shown for reactions (3) and (4) in Figure 5 and for reactions (5), (6), and (7) in Figure 6.

Over the entire temperature range studied, the $[O(^3P)]$ decays were exponential except for reactions (1) and (2) at T > 700 K. As T increased, in case of reactions (1) and (2), $[O(^3P)]$ decays became non-exponential with the initial part of the decay being faster than the tail. This curvature was reduced when O_2 (the photolyte) concentration was increased while keeping $[O(^3P)]_0$ the same. The curvature was unaffected by changes in flash energy, total system pressure, flow rate and benzene (C_6D_6) concentration. However, when a mixture of N_2O and N_2 were photolyzed using 193 nm (ArF laser) radiation to produce $O(^3P)$,

Table I.

Rate Constant Data for the Reactions of $O(^3P)$ with Benzenes and Toluenes.

Temperature °K	Benzene	Benzene-d_6	Toluene	Toluene-d_3
298	$1.19 \pm .19 \times 10^{-14}$		$7.14 \pm .89 \times 10^{-14}$	$8.60 \pm .93 \times 10^{-14}$
326			$1.15 \pm .31 \times 10^{-13}$	
364	$5.29 \pm .70 \times 10^{-14}$			
376		$5.97 \pm .68 \times 10^{-14}$		$2.36 \pm .23 \times 10^{-13}$
392		$9.79 \pm 1.08 \times 10^{-14}$		$2.85 \pm .27 \times 10^{-13}$
402	$1.28 \pm .13 \times 10^{-13}$		$3.43 \pm .30 \times 10^{-13}$	
417	$1.35 \pm .10 \times 10^{-13}$			
440		$1.55 \pm .14 \times 10^{-13}$		$4.40 \pm .42 \times 10^{-13}$
452	$2.39 \pm .21 \times 10^{-13}$		$6.12 \pm .51 \times 10^{-13}$	
484	$2.61 \pm .30 \times 10^{-13}$			$7.42 \pm .63 \times 10^{-13}$
492		$2.86 \pm .32 \times 10^{-13}$		
497	$4.21 \pm .36 \times 10^{-13}$		$9.96 \pm .85 \times 10^{-13}$	
522	$4.89 \pm .41 \times 10^{-13}$			
550			$1.43 \pm .16 \times 10^{-12}$	
556	$6.70 \pm .84 \times 10^{-13}$		$1.51 \pm .18 \times 10^{-12}$	$1.30 \pm .14 \times 10^{-12}$
560	$5.52 \pm .53 \times 10^{-13}$			
578		$7.15 \pm .73 \times 10^{-13}$		
604				$1.61 \pm .13 \times 10^{-12}$
620	$9.90 \pm 1.12 \times 10^{-13}$			
636		$9.39 \pm .76 \times 10^{-13}$		$2.02 \pm .21 \times 10^{-12}$
640			$2.41 \pm .20 \times 10^{-12}$	

Table I. (continued)

Rate Constant Data for the Reactions of $O(^3P)$ with Benzenes and Toluenes.

Temperature °K	Benzene	Benzene-d_6	Toluene	Toluene-d_3
660	$1.34 \pm .12 \times 10^{-12}$			
718	$1.63 \pm .16 \times 10^{-12}$			
724	$1.76 \pm .19 \times 10^{-12}$			$3.00 \pm .31 \times 10^{-12}$
729	$1.58 \pm .23 \times 10^{-12}$			
742	$2.02 \pm .17 \times 10^{-12\dagger}$			
749	$1.69 \pm .19 \times 10^{-12\dagger}$			
807		$1.83 \pm .23 \times 10^{-12}$	$4.23 \pm .64 \times 10^{-12}$	$2.99 \pm .34 \times 10^{-12}$
823	$2.28 \pm .22 \times 10^{-12*}$		$3.93 \pm .45 \times 10^{-12}$	
826	$2.48 \pm .35 \times 10^{-12*}$			
837	$2.58 \pm .48 \times 10^{-12\dagger}$		$3.90 \pm .37 \times 10^{-12}$	
867	$3.01 \pm .36 \times 10^{-12\dagger}$			
930			$5.06 \pm .64 \times 10^{-12}$	$3.59 \pm .42 \times 10^{-12}$

---

† Curved pseudo first order decays

* Laser photolysis (193 nm) of N_2O

Table II.

Rate Constant Data for the Reactions of O(^{3}P) with Xylenes.

Temperature °K	m-xylene	o-xylene	p-xylene
298	$4.19 \pm .46 \times 10^{-13}$	$2.23 \pm .22 \times 10^{-13}$	$2.25 \pm .26 \times 10^{-13}$
372	$1.07 \pm .11 \times 10^{-12}$	$5.91 \pm .59 \times 10^{-13}$	$6.29 \pm .78 \times 10^{-13}$
484	$2.58 \pm .34 \times 10^{-12}$	$1.69 \pm .18 \times 10^{-12}$	$1.57 \pm .18 \times 10^{-12}$
569	$3.75 \pm .42 \times 10^{-12}$	$2.57 \pm .34 \times 10^{-12}$	$2.75 \pm .27 \times 10^{-12}$
634	$4.79 \pm .32 \times 10^{-12}$	$3.65 \pm .44 \times 10^{-12}$	$4.09 \pm .46 \times 10^{-12}$
706	$7.78 \pm .89 \times 10^{-12}$	$5.58 \pm .82 \times 10^{-12}$	$5.94 \pm .66 \times 10^{-12}$
815	$1.13 \pm .12 \times 10^{-12}$	$9.26 \pm .93 \times 10^{-12}$	$9.40 \pm 1.06 \times 10^{-12}$
966	$1.54 \pm .19 \times 10^{-11}$	$1.41 \pm .15 \times 10^{-11}$	$1.38 \pm .16 \times 10^{-11}$

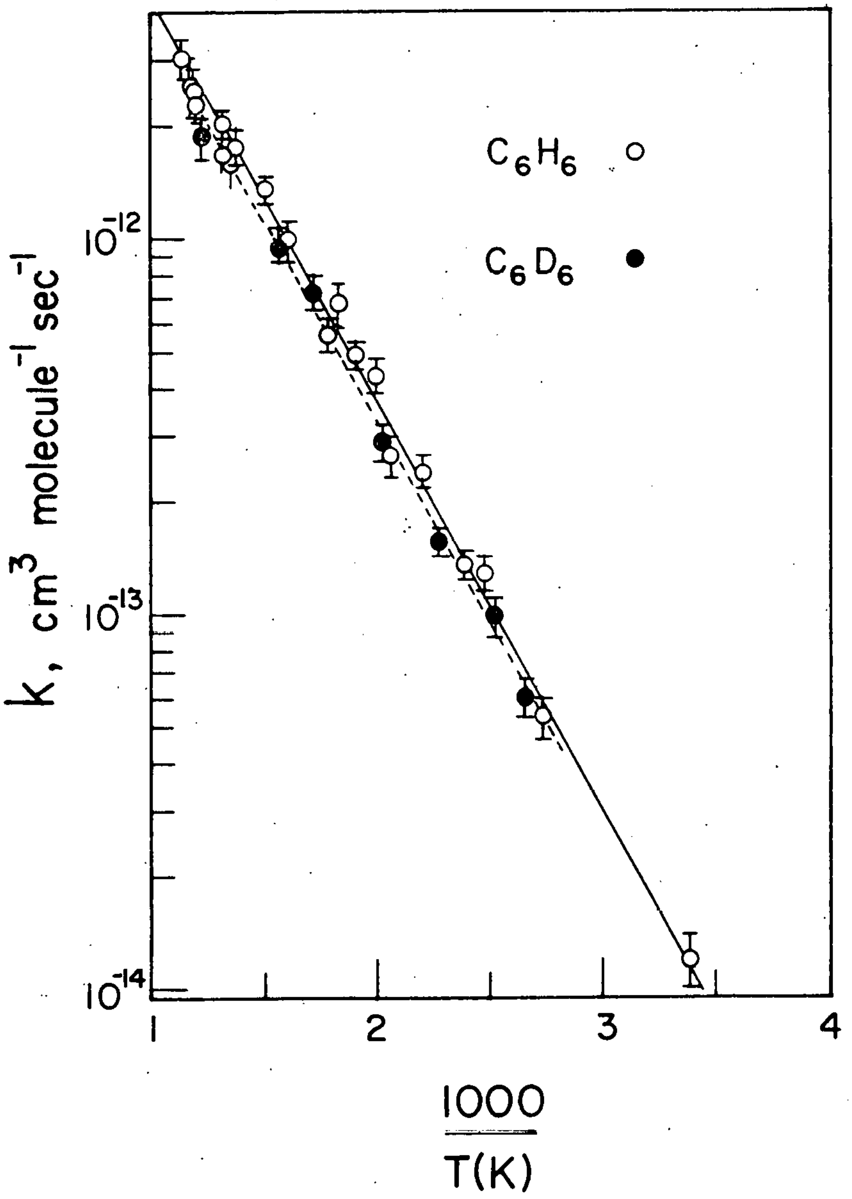

Figure 4. Arrhenius Plot of the Rate Constant for the Reaction of O(^{3}P) with C_6H_6 and C_6D_6.

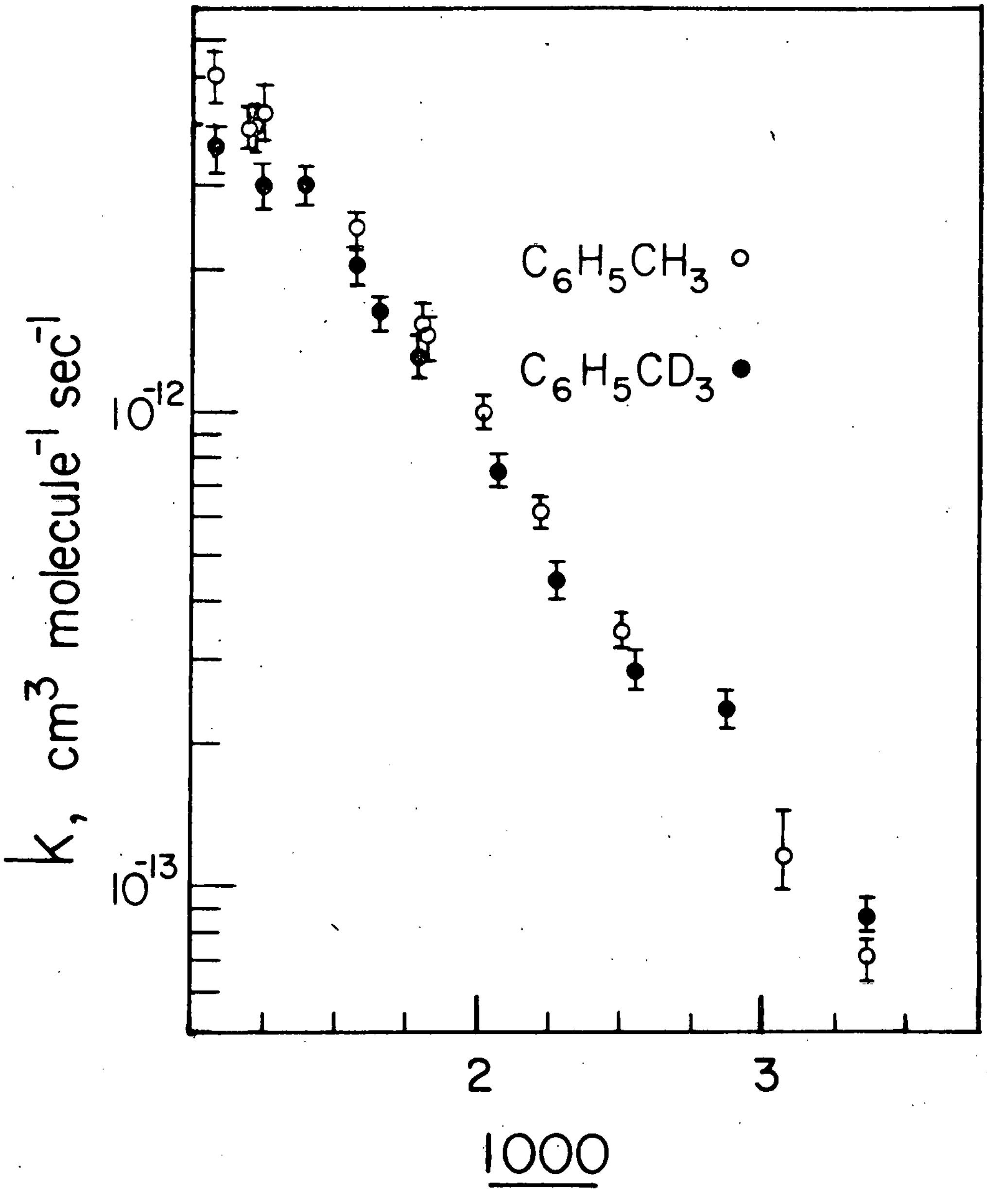

Figure 5. Arrhenius Plot of the Rate Constant for the Reaction of O(^{3}P) with $C_6H_5CH_3$ and $C_6H_5CD_3$.

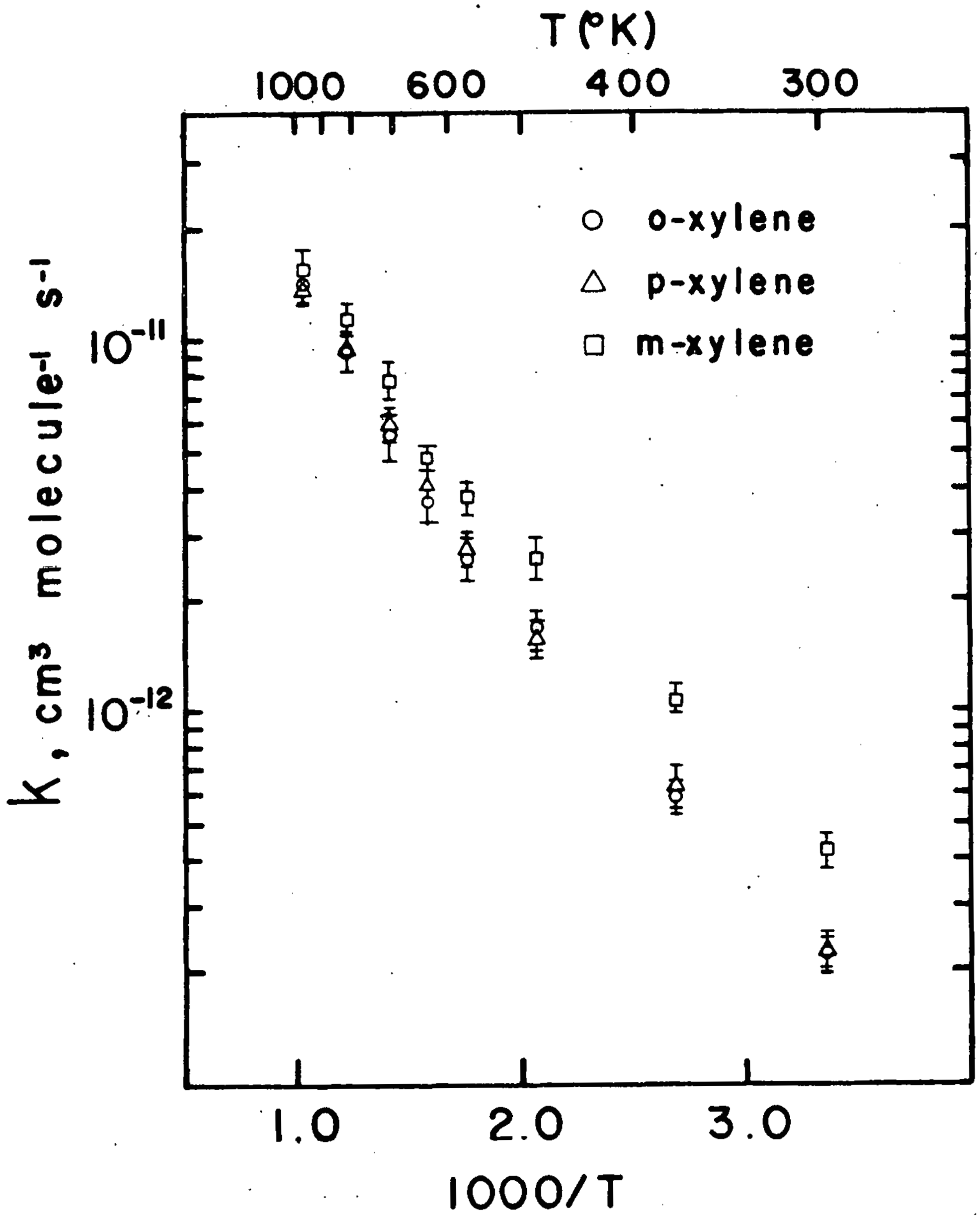

Figure 6. Arrhenius Plot of the Rate Constant for the Reaction of $O(^3P)$ with o-, m- and p-xylenes.

$$N_2O \xrightarrow{193\ nm} N_2 + O(^1D) \qquad (8)$$

$$O(^1D) + N_2 \rightarrow O(^3P) + N_2 , \qquad (9)$$

the $[O(^3P)]$ decays were exponential and the slope of these decays were identical to the initial slope obtained when O_2 photolysis was used as the source of $O(^3P)$. This observation clearly indicated that $O(^3P)$ was being formed, as the reaction progressed, via some secondary reaction of a species with O_2. [Of course, tests were carried out to ensure that indeed only $O(^3P)$ was being detected.] It will be later shown that this observation is consistent with the H atom being a product of reaction (1).

DISCUSSION

Figure 7 shows the results of $O(^3P)$ + benzene reactions obtained by all previous studies. It is clear that results of Bananno et al.[4] are clearly outside the error of the other four measurements. They had chemistry complications which could account for this discrepancy, our results are in reasonable agreement with that of the other investigations; the best agreement being with Colussi et al.[3] Our 298 K value of k_1 is the lowest that has been measured. It should be pointed out that the apparently different Arrhenius expressions derived from all four investigations converge aroud 450 K, the upper temperature limit of all previous investigations.

Based on the molecular beam studies of Sibener et al,[5] and Sloane,[6] it is clear the $O(^3P)$ reacts with C_6H_6 via addition to the ring.

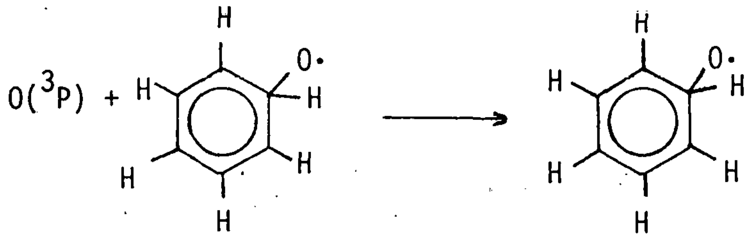

(10)

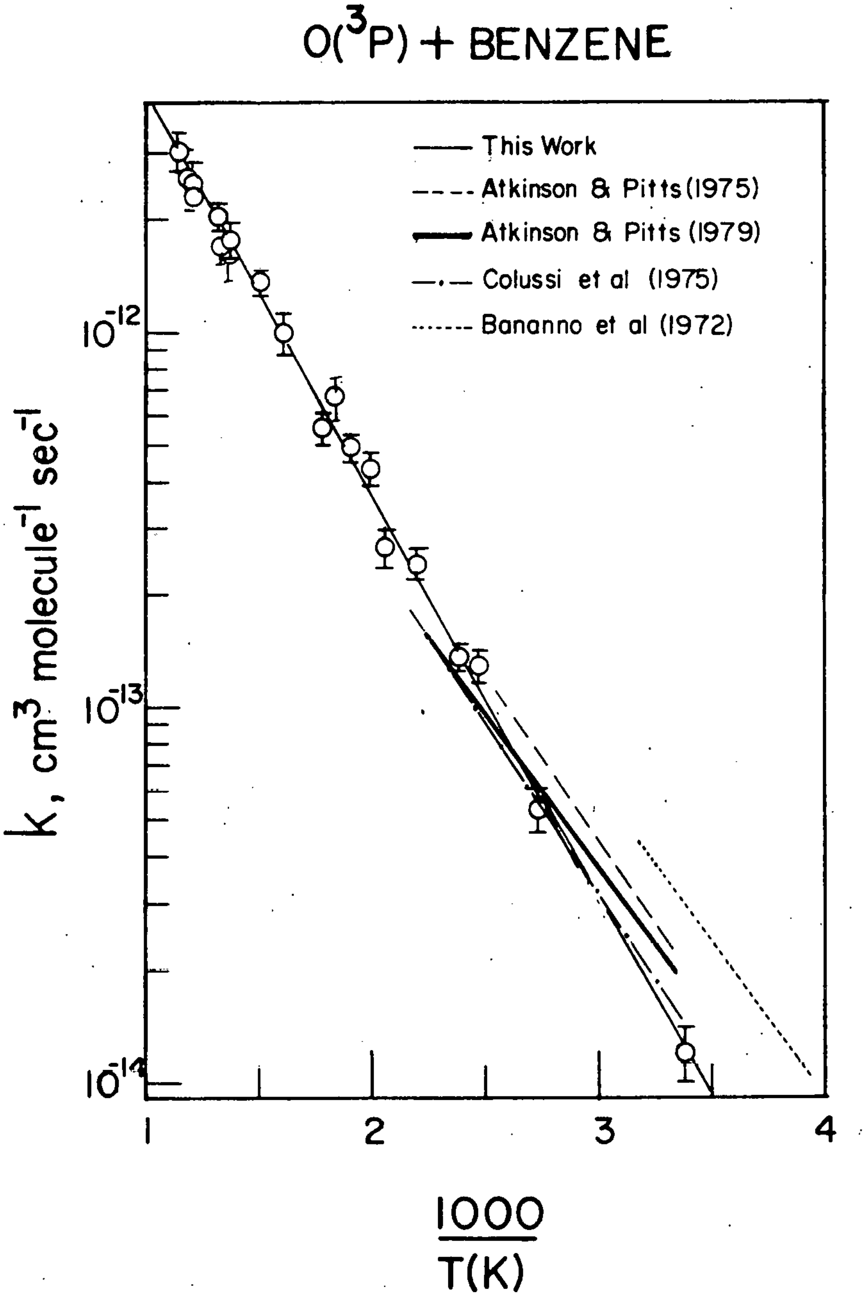

Figure 7. Comparison of k_1 with Results of Previous Investigations.

The adduct can either undergo rearrangement to form phenol,

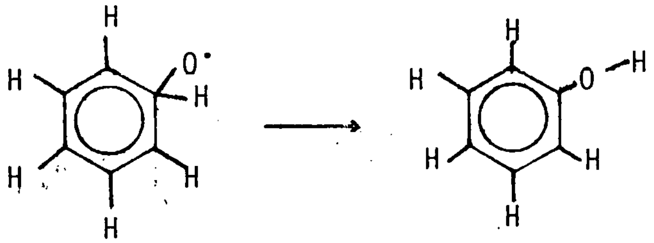

(11)

or eliminate the H atom,

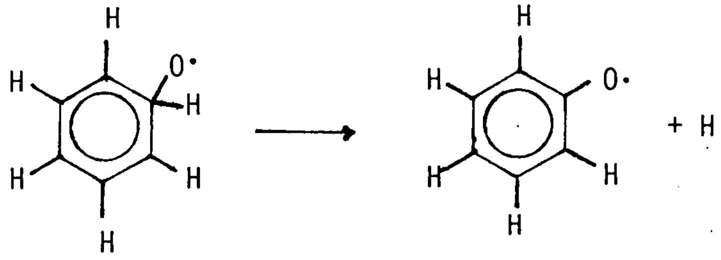

(12)

or eliminate CO,

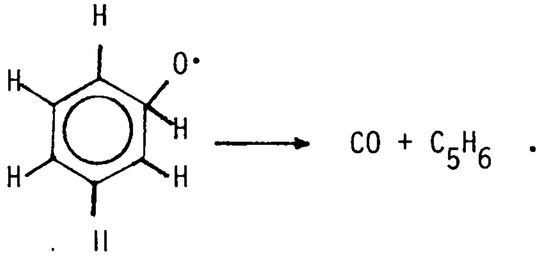

(13)

In variance of the rate constant for the reaction of $O(^3P)$ with benzene with the isotopic identity of hydrogen atom, (i.e., $k_1 = k_2$) shows that the primary step is addition of $O(^3P)$ to the ring and this confirms step 10 being the initial reaction. There is some controversy regarding step 13. Sloane claims to have seen CO, while Sibener et al.[5] do not. Also, Sibener et al. have pointed out that the origin of CO seen by Sloane[6] is probably dissociation of the parent ion in the mass spectrometer. To resolve this controversy, we tried to detect

CO via resonance fluorescence. We did not observe CO thereby, probably, confirming results of Sibener et al. It should, however, be remembered that our experimental conditions (e.g., pressure) are very different from those in beam studies. We have some indications for reaction (12) being a dominant channel. H atoms would, of course, be scavenged by O_2 in our system to form HO_2 at low temperatures. However, at high temperatures, this process slows down and H atoms can then react with benzene itself. At much higher temperatures, H atoms can react with O_2 to reform $O(^3P)$,

$$H + O_2 \rightarrow OH + O(^3P) \ . \tag{14}$$

Reaction (14), we believe, was the cause of curvature in $O(^3P)$ decay plots at high temperatures. As pointed out earlier, when N_2O was used as the $O(^3P)$ source, the curvature was not observed thereby adding further credence to our hypothesis. [We will, in the near future, follow H atom concentrations directly.]

Figure 8 shows the results of $O(^3P)$ + toluene reactions obtained by all previous studies. As in the case of benzene reactions the results are in reasonable agreement except for those of Furuyama and Ebara.[7]

All the reactions that can take place in the case of benzene can also occur with toluene. In addition, it is possible to have side-chain hydrogen abstraction at higher temperatures,

$$O(^3P) + C_6H_5CH_3 \longrightarrow C_6H_5CH_2{\cdot} + OH \ . \qquad (15$$

To check for the possibility, we carried out measurements of $O(^3P)$ reactions with $C_6H_5CD_3$, i.e., reaction (4). If side-chain hydrogen abstraction is significant, then k_4 would be smaller than k_3. As seen from Figure 5, $k_4 \simeq k_3$ thereby indicating that side-chain hydrogen abstraction is not very important in the temperature range studied.

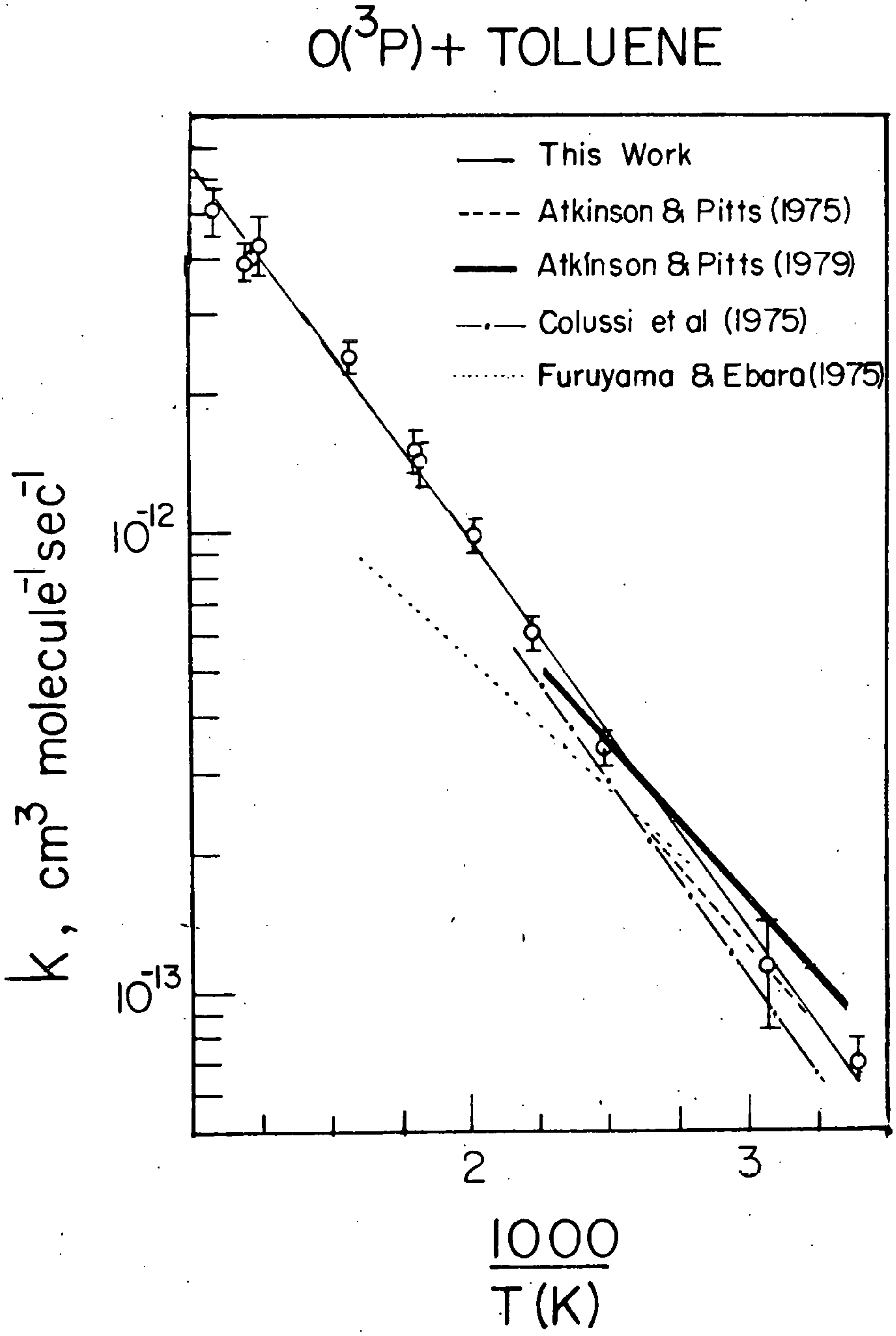

Figure 8. Comparison of k_3 with Results of Previous Investigations.

The results of reactions (5), (6), and (7) are shown in Figure 6 and Table II. The most interesting feature that is observed is that m-xylene reacts faster than o- or p-xylene with $O(^3P)$. This is identical to the reactions of OH since both $O(^3P)$ and OH are reacting with xylenes via electrophilic addition. Another feature that is observed is the slight curvature in Arrhenius plots. We are still working on this process and hence no conclusion can be drawn at this point.

Finally, for the sake of comparison, Table III lists Arrhenius parameters of all $O(^3P)$ reactions studied until now in our laboratory. It is clear that as substitution of the ring is increased, the reactivity of the compound with $O(^3P)$ increases and the activation energy decreases keeping the A factors approximately the same.

Table III.

Summary of Arrhenius Parameters

Reaction	$A \times 10^{11}$	-E/R	Temperature Range
$O(^3P) + C_6H_6$	5.11 ± 0.79	2467 ± 80	298 - 870 K
$O(^3P) + C_6D_6$	4.0 ± 1.4	2404 ± 80	298 - 806 K
$O(^3P) + C_6H_5CH_3$	4.2 ± 0.65	1900 ± 74	298 - 930 K
$O(^3P) + C_6H_5CD_3$	2.85 ± 0.71	1765 ± 121	298 - 930 K
$O(^3P)$ + o-xylene	3.99 ± 0.76	1550 ± 75	298 - 569 K*
$O(^3P)$ + m-xylene	4.36 ± 0.49	1381 ± 45	298 - 569 K*
$O(^3P)$ + p-xylene	4.02 ± 0.70	1548 ± 69	298 - 569 K*

---

*Above 569 K, slight curvature is observed and is therefore not included in this calculation.

REFERENCES

1. R. Atkinson and J.M. Pitts, Jr., J. Phys. Chem. 78, 1780 (1974).
2. R. Atkinson and J.M. Pitts, Jr., Chem. Phys. Lett. 63, 485 (1979).
3. A.J. Colussi, D.L. Singleton, R.S. Irwin, and R.J. Cvetanović, J. Phys. Chem. 79, 1900 (1975).
4. R.A. Bananno, P. Kim, J.H. Lee, and R.B. Timmons, J. Chem. Phys. 57, 1377 (1972).
5. S.J. Sibener, R.J. Buss, P. Casavecchia, T. Hirooka, and Y.T. Lee, J. Chem. Phys. 72, 4341 (1980).
6. T.M. Sloane, J. Chem. Phys. 67, 2267 (1977).
7. S. Furuyama and N. Ebara, Int. J. Chem. Kinet. VII, 689 (1975).